Supplementary Information

Chemically bonded interface modulated S-scheme charge transfer in Sb_2S_3@$ZnIn_2S_4$ core–shell heterostructures for boosted catalytic activity toward nitrogen photofixation

Cheng-Jie Zheng[a], Chen Zhang[a], Hao-Xiang Yang[a], Tingting Chen[a], Zhi-Cai He[a,*], Jian Zhang[b], Guo-Bo Huang[a,*], Mingyuan Wang[*,c], Guiwu Liu[d], Wei Chen[*,a]

[a]School of Pharmaceutical and Chemical Engineering, Taizhou University, Jiaojiang 318000, Zhejiang Province, PR China

[b]State Key Laboratory of Organic Electronics and Information Displays and Institute of Advanced Materials (IAM), New Energy Technology Engineering Lab of Jiangsu Province, Nanjing University of Posts and Telecommunications (NUPT), Nanjing 210023, Jiangsu, P. R. China

[c]School of Mechanical Engineering, Jiangsu University, Zhenjiang, 212013, Jiangsu, P. R. China

[d]School of Materials Science and Engineering, Jiangsu University, Zhenjiang 212013, China

Corresponding authors:

hezhicai@tzc.edu.cn (Z. He) gbhuang973@163.com (G.-B. Huang)

wmingyuan298@gmail.com (M. Wang) wchen@tzc.edu.cn (W. Chen)

Theoretical calculation

In this study, all calculations were conducted using density functional theory (DFT) as implemented in the Vienna Ab initio Simulation Package (VASP) [1]. The generalized gradient approximation (GGA) with the Perdew-Burke-Ernzerhof (PBE) functional was employed to describe the exchange-correlation interactions [2]. The ion-electron interactions were treated using the projector-augmented wave (PAW) method [3]. Van der Waals (vdW) interactions were accounted for using the DFT-D3 method to accurately describe the interactions between the substrate and gas molecules [4]. To avoid spurious interactions arising from periodic boundary conditions, a vacuum layer of at least 15 Å was introduced in the unit cell [5]. The plane-wave cutoff energy was set to 400 eV, and the Brillouin zone was sampled using a 3×3×1 k-point grid. The convergence criteria for energy and force were set to 10^{-4} eV per atom and 0.02 eV/Å, respectively.

The Gibbs free energy was calculated by adopting the standard hydrogen electrode model [6,7]:

$$\Delta G = \Delta E + \Delta E_{ZPE} \quad T\Delta S$$

Where ΔE, ΔE_{ZPE}, and ΔS are the adsorption energy, changes in zero-point energy and entropy, respectively. ΔE_{ZPE} and ΔS are calculated by vibration frequency. T is temperature (298.15 K). The ΔE, ΔE_{ZPE}, and ΔS were calculated through the equation:

$$\Delta E = \Delta E_{total} \ \ E_{surface} \ \ E_{gas}$$

$$E_{ZPE} = \tfrac{1}{2}\Sigma_i h\nu_i$$

$$TS = K_B T \Sigma_i \ln\{1 \ \ e\, h\nu_i / K_B T\} \ \ \Sigma_i h\nu_i \{1/(e\, h\nu_i / K_B T)\}$$

Where E_{total}, $E_{surface}$, and E_{gas} are the total energies for different adsorption sites, substrate slab, and adsorbent, respectively. The symbols h and ν represent Planck's constant and the vibrational frequency, respectively. Only the vibrational modes of the adsorbate were explicitly calculated, while the catalyst sheet was kept fixed. The Boltzmann constant is denoted as K_B.

Preparation of photoelectrode

The detailed preparation process of photoelectrode can be described as follows. The fluoride-tin oxide (FTO) glass provided by Zhuhai Kaivo Optoelectronic Technology Co., Ltd was used to prepare the working electrode, which was first washed by a 100 W ultrasonic wave (KQ-100DE) in ethanol for 30 min and dried at 333 K. 10 mg of samples were uniformly dispersed in 5 mL of mixed solvent ($V_{\text{ultrapure water}}$:$V_{\text{isopropanol}}$:$V_{\text{5 wt\% Nafion solution}}$ = 40:20:1) by a 100 W ultrasonic wave for 30 min to disperse it evenly to obtain a uniform suspension. Then, 0.1 mL of above suspension was dropwisely added on the washed FTO glass, which was placed on heating plates with heating temperature of 333 K until the solvent was completely evaporated to obtain the working electrode.

Synthesis of Au loaded Sb_2S_3@$ZnIn_2S_4$ sample

Au loaded Sb_2S_3@$ZnIn_2S_4$ sample was synthesized by in situ photo-deposition of Au nanoparticles onto Sb_2S_3@$ZnIn_2S_4$ sample. Typically, 50 mg Sb_2S_3@$ZnIn_2S_4$-75 sample was suspended in 40 mL $HAuCl_4 \cdot 3H_2O$ solution with initial concentration of 0.5 $g \cdot L^{-1}$. After ultrasound treatment for several minutes, 10 mL methanol was added into above suspension as a sacrificial agent of photogenerated holes. Subsequently, the above suspension was irradiated by a 300 W Xe lamp for successive 90 min. Finally, Au loaded Sb_2S_3@$ZnIn_2S_4$ sample was collected by washing with deionized water two times and absolute ethanol three times, and drying in an oven at 60 ^{o}C for 6 h.

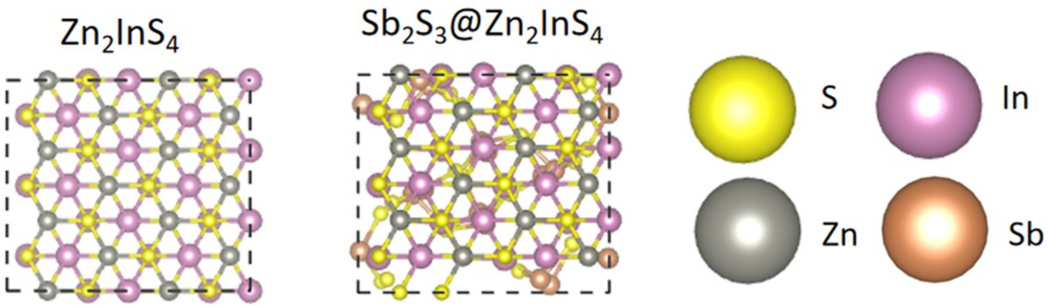

Fig. S1 Atomic structure diagram of $ZnIn_2S_4$ and $Sb_2S_3@ZnIn_2S_4$.

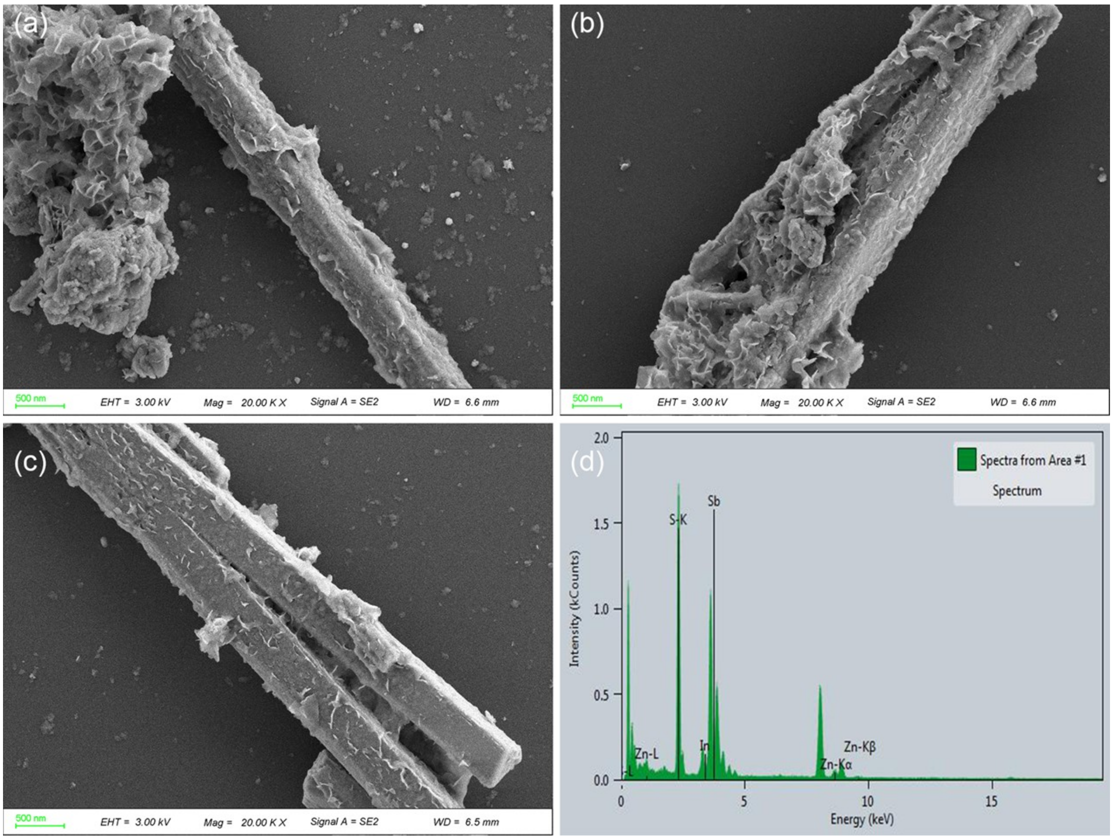

Fig. S2 SEM images of (a) $Sb_2S_3@ZnIn_2S_4$-25, (b) $Sb_2S_3@ZnIn_2S_4$-50, (c) $Sb_2S_3@ZnIn_2S_4$-100, and (d) EDX spectrum of $Sb_2S_3@ZnIn_2S_4$-75.

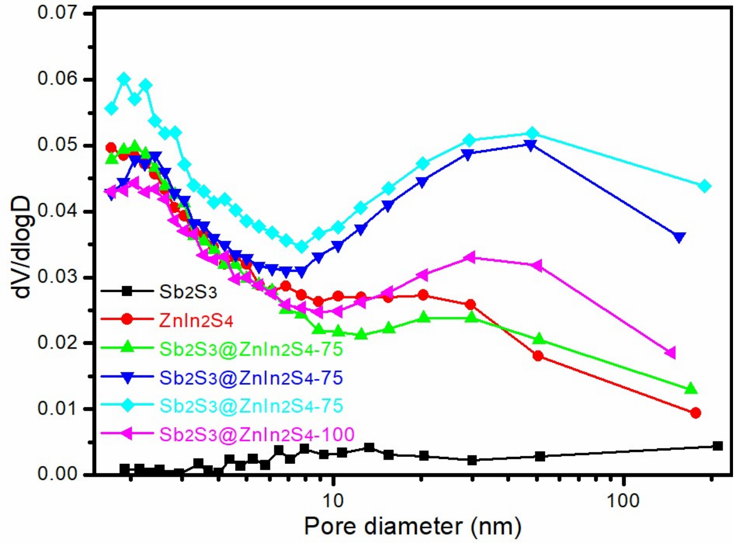

Fig. S3 Pore size distribution of pure $ZnIn_2S_4$, bare Sb_2S_3 and their $Sb_2S_3@ZnIn_2S_4$ core-shell heterostructures

Table S1. Surface area, pore diameter and pore volume parameters for bare Sb_2S_3, pure $ZnIn_2S_4$ and the $Sb_2S_3@ZnIn_2S_4$ samples.

Samples	Surface area[a] (m^2/g)	Pore size[b] (nm)	V_t^c (cm^3/g)
Sb_2S_3	2.011	11.713	0.0630
$ZnIn_2S_4$	45.340	4.932	0.0612
$Sb_2S_3@ZnIn_2S_4$-25	43.349	4.915	0.0607
$Sb_2S_3@ZnIn_2S_4$-50	46.717	7.539	0.0998
$Sb_2S_3@ZnIn_2S_4$-75	54.234	7.100	0.112
$Sb_2S_3@ZnIn_2S_4$-100	38.266	6.052	0.0696

[a] Measured using N_2 sorption with the BET method.

[b] Diameter size of porous structure calculated using the N_2 desorption with Barrett-Joyner-Halenda (BJH) method.

[c] Total pore volume of pores estimated at P/P_0 approaching 0.99.

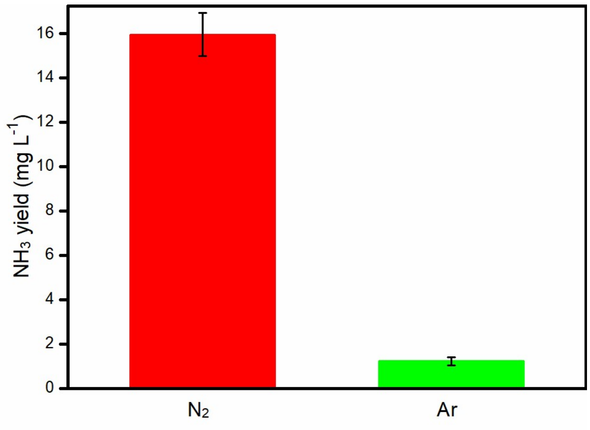

Fig. S4 Catalytic activity toward nitrogen photofixation in different atmosphere.

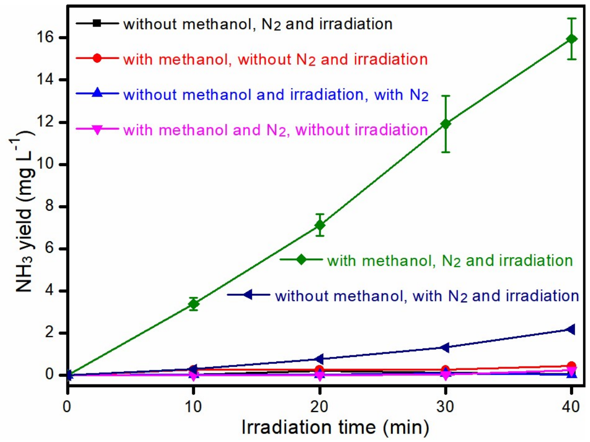

Fig. S5 Catalytic activity of control experiments over Sb_2S_3@$ZnIn_2S_4$-75 toward nitrogen photofixation.

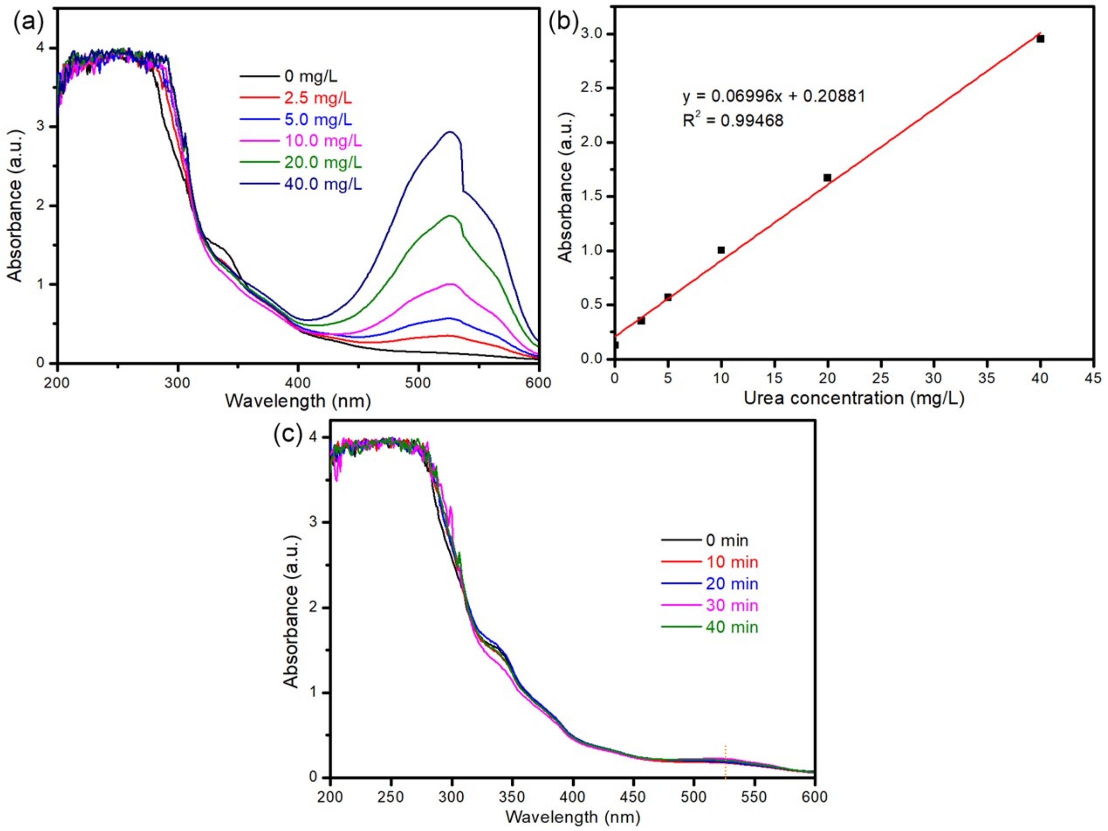

Fig. S6 (a) UV-Vis absorption spectra and (b) plotting of standard curves of different-concentration urea solutions detected by diacetyl monoxime method, and (c) UV-Vis absorption spectra of reaction liquid obtained from different irradiation time of visible light.

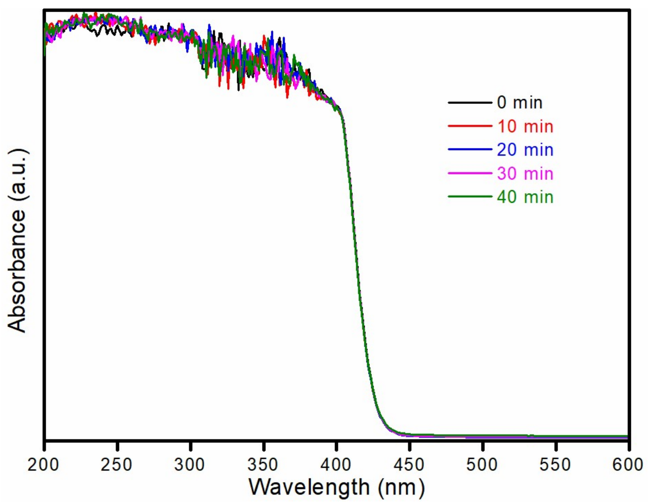

Fig. S7 UV-vis absorption curves of reaction solution obtained from different N_2 photofixation process after adding Watt and Chrisp reagent.

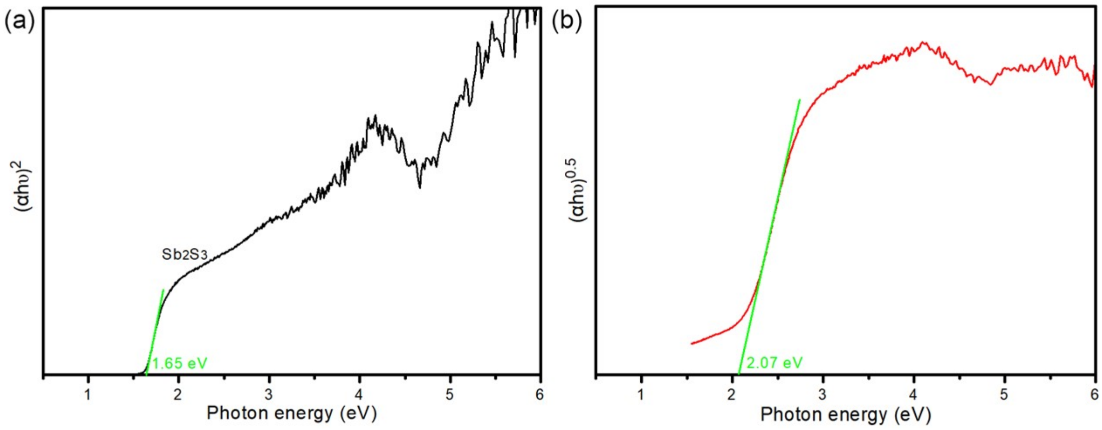

Fig. S8 Band gap of (a) Sb_2S_3 and (b) $ZnIn_2S_4$.

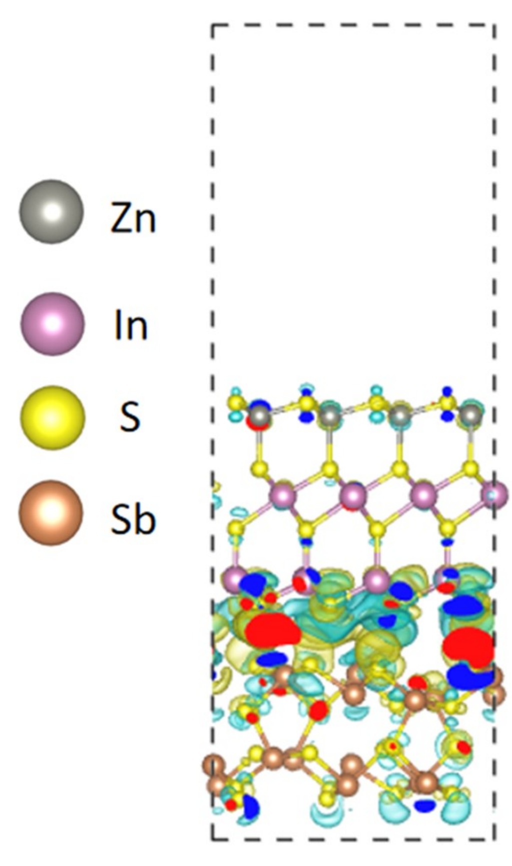

Fig. S9 Charge density difference of the Sb_2S_3@$ZnIn_2S_4$ model. Yellow represents charge accumulation and cyan represents charge depletion.

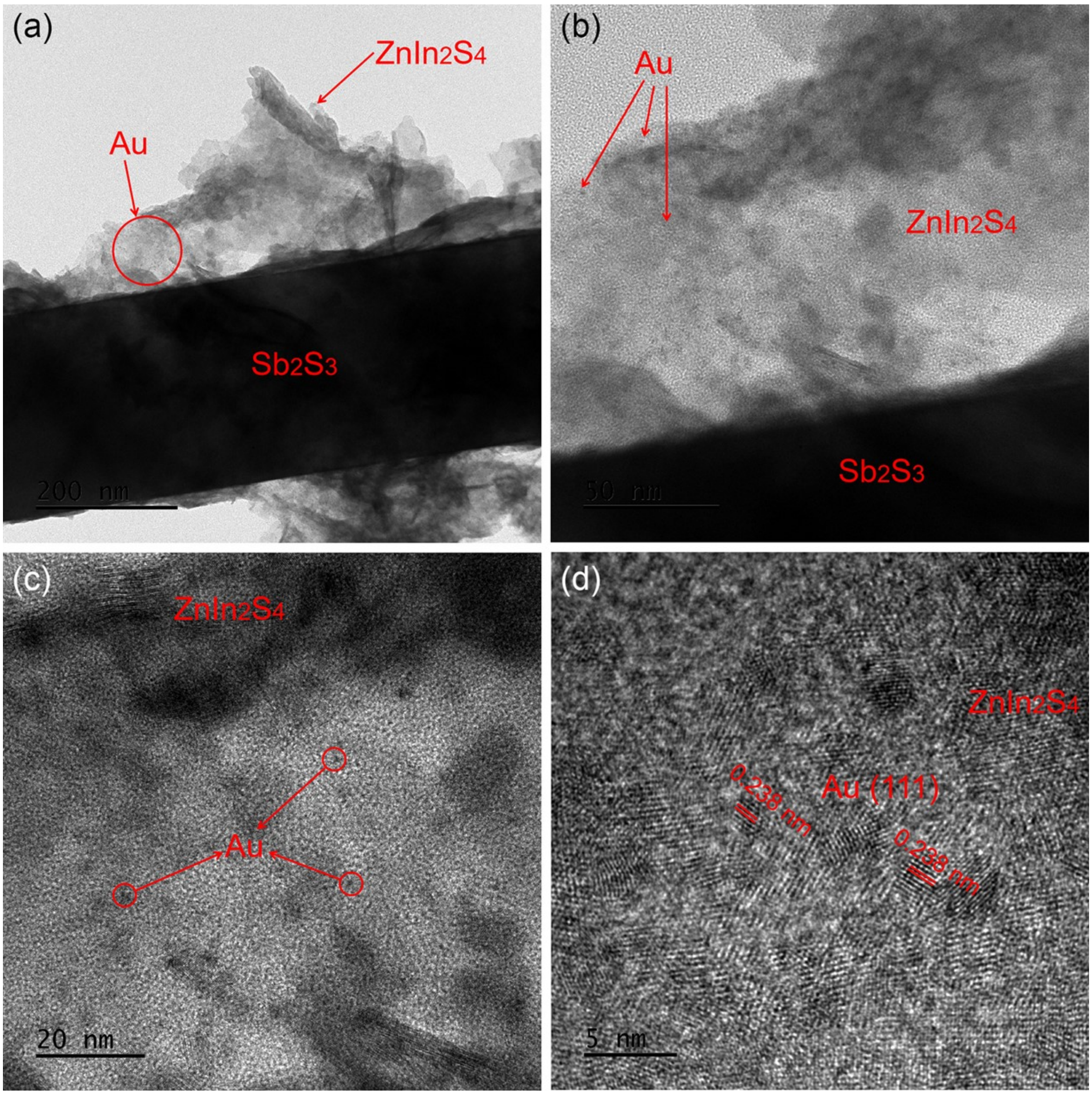

Fig. S10 (a,b) TEM images and (c,d) HRTEM images of Au loaded Sb_2S_3@$ZnIn_2S_4$-75 sample.

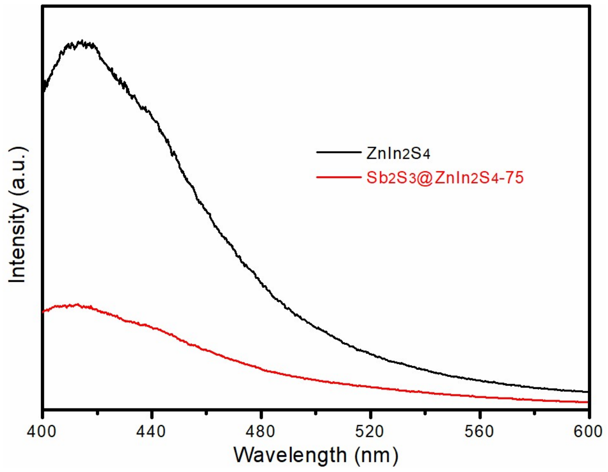

Fig. S11 PL spectra of $ZnIn_2S_4$ and Sb_2S_3@$ZnIn_2S_4$-75 sample.

Table S2 Corresponding kinetic fitted results of $ZnIn_2S_4$ and Sb_2S_3@$ZnIn_2S_4$-75 within 30 ns.

Samples	A_1	τ_1 (ns)	A_2	τ_2 (ns)	τ_{ave} (ns)
$ZnIn_2S_4$	0.487	2.52	0.273	6.39	4.81
Sb_2S_3@$ZnIn_2S_4$-75	0.700	2.84	0.117	9.97	5.48

References

1 G. Kresse and J. Furthmuller, *Phys. Rev. B: Condens. Matter Mater. Phys.*, 1996, **54**, 11169-11186.

2 J. P. Perdew, K. Burke and M. Ernzerhof, *Phys. Rev. Lett.*, 1996, **77**, 3865–3868.

3 G. Kresse and D. Joubert, *Phys. Rev. B: Condens. Matter Mater. Phys.*, 1999, **59**, 1758-1775.

4 S. Grimme, *Comput. Chem.*, 2006, **27**, 1787-1799.

5 L. Seixas, A. Carvalho and A.H.C. Neto, *Phys. Rev. B: Condens. Matter Mater. Phys.*, 2015, **91**, 155138.

6 H. Yang, Y. Wu, G. Li, Q. Lin, Q. Hu, Q. Zhang, J. Liu and C. He, *J. Am. Chem. Soc.*, 2019, **141**, 12717-12723.

7 M. Wang, Z. Xu, X. Zhang, J. Yang, J. Liu, G. Qiao and G. Liu, *Appl. Surf. Sci.*, 2021, **554**, 149614.